Compact medical fluorosensor for minimally invasive tissue characterization

af Klinteberg, C; Andreasson, M; Sandstrom, O; Andersson-Engels, Stefan; Svanberg, Sune

Published in:
Review of Scientific Instruments

DOI:
10.1063/1.1867569

2005

Compact medical fluorosensor for minimally invasive tissue characterization

Claes af Klinteberg, Markus Andreasson, Ola Sandström,
Stefan Andersson-Engels, and Sune Svanberg[a)]
Department of Physics, Lund Institute of Technology P.O. Box 118, SE-221 00 Lund, Sweden

(Received 15 August 2002; accepted 22 December 2004; published online 2 March 2005)

A compact fiber-optic point-measuring fluorosensor fully adapted to clinical studies is described. The system can use two excitation wavelengths, 337 and 405 nm, obtained from a nitrogen laser directly, or after dye laser conversion, respectively. The image intensifier used in the spectrometer can be gated with a variable time delay, allowing also time-resolved spectra to be extracted, with a time resolution of about 4 ns. Moreover, diffusely scattered white light can be spectrally recorded. The system is fully computer controlled enabling short recording times in clinical application, which are illustrated. © *2005 American Institute of Physics.* [DOI: 10.1063/1.1867569]

I. INTRODUCTION

Various optical spectroscopy techniques have been investigated in recent years in the search for minimally or noninvasive methods to guide medical examinations. Among these techniques, fluorescence spectroscopy is presently one of the most studied and promising alternatives for identifying premalignant and malignant tumors, but also atherosclerotic plaques.

The basis for fluorescence investigations is the excitation of molecules and the subsequent examination of the reemitted light. Measurable fluorescence properties useful for the identification of molecules and their concentrations include the excitation and emission spectra, and the excited state lifetime. In tissue many fluorophores are present, and the fluorescence signal will thus be a superposition of several contributions. Tissue characterization utilizing fluorescence techniques is based on differences in molecular contents between different tissue types. Both excitation and emission spectra have broad features for molecules in solids and liquids, due to intermolecular interactions smoothening any sharp structures. The possibilities to characterize tissue types can in some applications be enhanced by the use of exogenous fluorescent markers. The development of fluorescence techniques for tissue characterization was initiated in the early 1960's by the observation that malignant tumors could be visualized by the red fluorescence emission following violet light illumination, if a haematoporphyrin derivative was first given to the patient.[1] This observation was later employed by Profio and Doiron developing the instruments to efficiently detect the faint fluorescence emission.[2] During the last decade, many investigators have studied fluorescence to evaluate its clinical potential.

Many groups, including our own, have assembled systems utilizing off-the-shelf research equipment, often including a laser to produce the excitation light and a spectrometer connected to a charge-coupled device (CCD) camera for detection, for clinical point-wise investigations of the fluorescence emission from tissue.[3–10] Using violet diode lasers and small spectrometers, it has become possible to construct very small fluorescence instrumentation.[11] The studies performed to date with this type of equipment have been very valuable to evaluate the potential of fluorescence as a diagnostic tool, and to identify applications, that could benefit from this technique.

Other studies have been aiming at developing fluorescence imaging systems to scan larger tissue surfaces to detect small lesions of malignant growth.[12–24] Images are also much easier to interpret for the examining doctor than results presented from selected positions. For some applications exogenous substances providing high fluorescence signals can be utilized. One example is the local application of δ-aminolevulinic acid (ALA), yielding the strongly fluorescent protoporphyrin IX (PpIX). This can be used to visualize malignant tumors in, for instance, the urinary bladder during cystoscopy.[15]

A common problem for both point-monitoring and imaging systems is how to enable simultaneous fluorescence measurements and white light examination. This can be achieved if pulsed fluorescence excitation and synchronized gated detection is performed.

Tissue characterization, based on time-resolved fluorescence spectroscopy and imaging, has also been employed by a few groups.[25–28] This is possible by using the capability of the image intensified CCD cameras to be gated with a short gate width. This technique utilizes another dimension in the analysis of tissue, the fluorescence lifetime. For further information regarding tissue fluorescence studies performed, we refer to a number of review papers covering this topic.[29–37]

The aim of the present work was to utilize the long experience in our group dating back to the early 1980's[38] regarding fluorescence techniques for tissue characterization, to develop a point-measuring fluorosensor fully adapted to clinical studies. Although imaging systems generally are superior for many applications, compact point-measuring fluorosensors will still be very useful, for instance for continued evaluation in numerous clinical applications and as an aid in

[a)]Electronic mail: sune.svanberg@fysik.lth.se

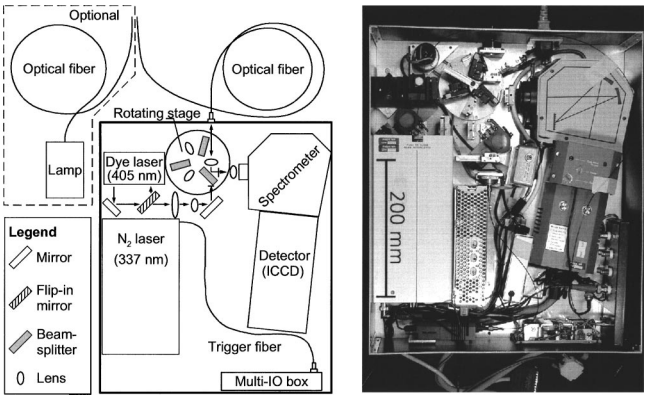

FIG. 1. (a) Schematic illustration of the design of the fluorosensor and (b) photograph of the system.

deciding where and whether biopsies should be collected. The system should be flexible and extract the fluorescence information in an optimal way. This has been realized by employing differences in fluorescence excitation as well as emission and lifetime. Our system has been designed to be compact and fully computer controlled, enabling short recording times in clinical applications, which are illustrated.

II. SYSTEM DESCRIPTION

The fluorosensor has the possibility of measuring time-gated fluorescence spectra following excitation with two different excitation sources. It is designed to utilize also a third beam path, providing the additional feature of employing scattered white light for tissue characterization. A unique feature of the system is its compactness. The size of the optical unit is $47\times40\times21$ cm^3 and the weight is 19 kg. This corresponds to a reduction in volume by a factor of 20 compared to our earlier system,[5,39] while extending the performance greatly. A schematic illustration of the optical unit design is shown in Fig. 1(a), while a photograph of the interior of the system is shown in Fig. 1(b).

A. Light sources

The excitation light is provided by a small sealed-off nitrogen (N_2) laser (Laser Science, Franklin, MA, VSL-337) or a dye laser pumped by the N_2 laser (a modified Laser Science DLM-110). The N_2 laser emits 3-ns-long light pulses at 337 nm. The pulse energy is approximately 75 μJ and it runs at 15 Hz. The small dye laser does not have any wavelength selective optical components and will thus lase at the peak emission wavelength of the dye. The wavelength can therefore be selected by the choice of dye only. Frequently, the dye 4,4′-diphenylstilbene (Exciton DPS) emitting at 405 nm is used for this system. This is of interest as porphyrins are optimally excited at this wavelength. The dye laser provides approximately 10 μJ pulses at 405 nm.

When using the N_2 laser for fluorescence excitation, the laser light is first redirected 90 deg using a multilayer coated mirror (Melles Griot, Rochester, NY) in a motorized flip-in mount (New Focus, San Jose, CA, 8891M). The beam is then transformed in a telescope to reach a diameter matching the optics. The telescope consists of two biconvex fused silica lenses (CVI) with focal lengths 27 and 19 mm, respectively. Both lenses are antireflection (ar) coated for 337 and 405 nm. The light is again reflected 90 deg with a mirror identical to the first one.

The beam now enters the optics mounted on a rotational stage. The first component is a narrow band pass filter (ESCO Products, Oak Ridge, NJ, S903400) transmitting the laser light while suppressing plasma emission lines from the discharge in the laser cartridge. The center wavelength of the filter is 340 nm, its full width at half maximum (FWHM) is 10 nm, and its transmission 35%. The filtered laser light will then pass through a broadband 50/50% beam splitter (EKSMA), specified for wavelengths between 400 and 1000 nm separating the excitation and emission beam paths. We considered using a more light-efficient dichroic beam splitter instead of the broadband unit chosen. The commercially available dichroic beam splitters have a steep transition between reflected and transmitted wavelengths but also exhibit a nonflat transmission profile. In our experience, this uneven transmission profile is difficult to compensate for in a reliable way, when analyzing recorded spectra. The laser light is then further collimated by a biconvex fused silica lens ($f=60$ mm, $\varnothing=12.5$ mm; CVI).

A 600-μm core diameter fused silica optical fiber (Fiberguide Ind., Stirling, NJ, SFS600N) is used to guide the excitation light to the tissue under examination. The fiber is connected to the side of the system housing using a SMA-type connector attached to an adjustable fiber port [Optics for Research (Caldwell, NJ, custom specific model PAF-XM-5-NUV-Z)]. The focusing of the light is matched to the numerical aperture 0.22 of the optical fiber.

The clear-cut, polished distal end of the fiber is used in gentle contact with the tissue. As the excitation light enters the tissue, it is quickly attenuated and the penetration depth is of the order of a few hundred micrometers. A fraction of the absorbed light will generate reemission of fluorescence light. The same optical fiber collects some of the fluorescence and guides it back to the instrument. The lens used to focus the excitation light into the fiber also collimates the fluorescence light exiting the fiber. The broadband beam splitter reflects about half of the fluorescence light toward the spectrometer. A 2-mm-thick colored-glass filter (Schott GG385) blocking any scattered laser light is mounted on the rotational stage next to the beam splitter. This high-pass filter transmits 10%, 50%, and 90% at the wavelengths 375, 385, and 410 nm, respectively.

When the dye laser is used for excitation, the first mirror is flipped down. The distance between the out-coupling window of the N_2 laser and a cylindrical lens focusing the light onto the dye cuvette in the dye laser is 60 mm. This distance cannot be much longer, or the output of the dye laser will drop drastically. A mirror inside the dye laser is repositioned to direct the beam toward the N_2 laser. Another high reflecting multilayer mirror of the same type as above is directing the beam to the telescope, and further to the rotational stage. Before using the dye laser, the rotational stage is rotated to exchange the optics to the set used for excitation at 405 nm. The rotation is motorized and under computer control. The set of optics is exchanged in less than one second. For this

wavelength, no band-pass filter is needed, and the filter suppressing scattered laser light is exchanged to one with a longer cut-off wavelength (Schott GG 435). This high-pass filter transmits 10%, 50%, and 90% at the wavelengths 420, 435, and 465 nm, respectively.

B. Diffusely reflected white light

The diffuse reflectance of continuous wave white light can also be investigated. For this purpose, the illumination and detection must be performed with different fibers. The light from a small-sized tungsten halogen light source (Ocean Optics, Orlando, FL, LS-1-LL), seen at the bottom left part of the photograph in Fig. 1(b), is guided to the tissue by an optical fiber identical to the one described above, which now serves for detection only. The two fibers are mounted together with a center-to-center distance of 1 mm. A small fraction of the scattered light is collected by the detection fiber. The optics used in the detection system can be the same as for 337 nm excitation. If wavelengths below the 385 nm color filter cutoff are also to be included, the rotary stage can be turned to its third, filter-free position.

C. Detection system

The fluorescence light is then focused onto the 100-μm-wide entrance slit of a small-sized spectrometer (Oriel, Darmstadt, Germany, MS125) using a biconvex fused silica lens ($f=30$ mm, $\varnothing=12.5$ mm; CVI). The wavelength resolution of the spectrograph is 21 nm per mm with a 400 lines per mm grating blazed at 500 nm. The light is detected using an intensified charge-coupled device (CCD) camera having 1024×128 pixels (Andor Technology, Belfast, Northern Ireland, DH501-25U-01). The camera is thermoelectrically cooled and is usually operated at a temperature of 1 °C. The photocathode is of type W, and the minimum gating time is 1.8 ns. This detection system resulted in a spectral resolution FWHM of 2.2 nm and a detected wavelength range up to 805 nm.

D. Equipment synchronization

The synchronization of a recording is slightly different for time-integrated and time-gated measurements. In both cases the computer sends a pulse triggering the laser. Once the laser is firing, some laser light is picked up by an optical fiber at the output window of the N_2 laser. The fiber guides the light to a photodiode in a box of electronics used for synchronization purposes—the multi-IO box. For time-integrated measurements a 100-ns-long gate signal is generated in the multi-IO box. This signal is used to open the gate of the intensified CCD camera. Since the gate of the detector is open only 100 ns for each laser pulse, the ambient light is suppressed by more than a factor of 10^5, allowing the instrument to operate also in an environment with bright ambient light. The choice of a comparatively long gate time is motivated by making the system a little sensitive to the exact gating in standard, time-integrated measurements.

To make time-resolved measurements, one has to rearrange the hardware slightly. A high precision delay generator (Stanford Research Systems, Sunnyvale, CA, DG535) is presently needed to deliver delayed gate pulses to the detector. The triggering signal, generated in the multi-IO box, now trigs the delay generator, which in turn controls the image intensifier of the CCD camera. Since the delay generator has an intrinsic delay of approximately 85 ns, the system fiber is now extended with a 15-m-long delay fiber. The delay generator may be replaced by a set of fixed delays.

E. User interface

An application-specific software was developed to have a fully computer controlled data acquisition. A simple graphical user interface was designed to allow use by nonspecialists. Much effort was spent on reducing the number of user interactions with the system during routine measurements. This work has simplified and speeded up such measurements considerably. A graphical development environment, LabVIEW™ (National Instruments, Austin, TX), designed for instrument control and data acquisition, was utilized in this work. Software drivers supplied with the detector, including functions controlling all aspects of the camera, were used in the programming. The instrument is controlled by a panel-PC (Advantech PPC 150TT). The user-interface can be operated via the touch screen of the computer.

F. Recording procedure

In clinical recordings, both excitation wavelengths are usually utilized. Two fluorescence spectra are thus obtained from each measuring site in a sequence fully controlled by the computer software. At the beginning of a series of measurements, two background spectra, one for each excitation wavelength, are recorded and stored. The fiber probe is then positioned in the air far from anything that could fluoresce. Once this is done, the fiber can be positioned in gentle contact with the tissue, and the recordings start. Normally the signals from 20–60 laser pulses are accumulated and stored automatically. Such a set of recordings takes approximately 3–9 s, depending on the number of laser pulses being accumulated. Both spectra will immediately be displayed on the computer screen. After completion, the fiber can be moved to another position and a new pair of spectra can be recorded.

G. Calibration

The wavelength scale of the spectrometer is calibrated using the different peaks from a spectral calibration lamp or a fluorescent discharge lamp. After entering the correct nominal wavelength numbers a linear regression yields the wavelength scale.

The sensitivity of the system is wavelength dependent, but stable in time. A sensitivity calibration must therefore occasionally be made by recording the emission spectrum from a National Institute of Standards and Technology-traceable blackbody radiator. By dividing the tabulated emission profile with the recorded one, a correction curve is obtained. All spectra recorded by the system are then multiplied by this response curve before evaluation.

To allow comparisons of the intensity detected at different occasions, the signal from a fluorescence reference is

measured for both excitation wavelengths in connection with all investigations. Our reference consists of an optically thick sample of 10 mg rhodamine 6G (Rh6G) dissolved in 60 ml ethylene glycol in a quartz cuvette stored in the dark to avoid aging effects due to photobleaching. The overall sensitivity of the system might change slightly, due to contamination of the fiber tip and, if more than one probe fiber is used, differences in their transmission properties, as well as any instability of the excitation source or optics positioning. When analyzing recorded spectra, they are normalized to the corresponding fluorescence reference measurement.

H. System characterization measurements

Several measurements have been performed in order to characterize the performance of the system. The noise of the system was measured as the standard deviation over 20 pixels when subtracting the curves obtained from two sequential recordings. We measured the noise in both the background, i.e., the signal recorded while the fiber probe was held in air, and in the signal itself. The background noise mainly originated from statistical fluctuations in the detector dark current and in weak signals induced in the optics itself, while the noise in the signal mainly was due to photon statistics.

The sensitivity of the system was measured with reference to our internal fluorescence intensity standard mentioned above, and to normal Caucasian skin. Signal-to-noise ratios were evaluated in both cases.

In order to evaluate the time resolution by the system, a sequence of time-gated spectra was recorded from two samples: our rhodamine fluorescence intensity standard and photofrin dissolved in methanol, with a known lifetime of 15 ns.[40] The leading edge of the time gates for all the spectra was fixed in time so that the detector was opened well before the laser excitation pulse. The trailing edge was moved stepwise toward longer decay times for each subsequently recorded spectrum. This yielded a sequence of spectra with more and more of the fluorescence decay included. By integrating the signals under the peaks around 575 and 630 nm for rhodamine and Photofrin, respectively, two integrated fluorescence intensity curves could be plotted versus the detector gate width. By differentiating these curves, the fluorescence decay curves were obtained.

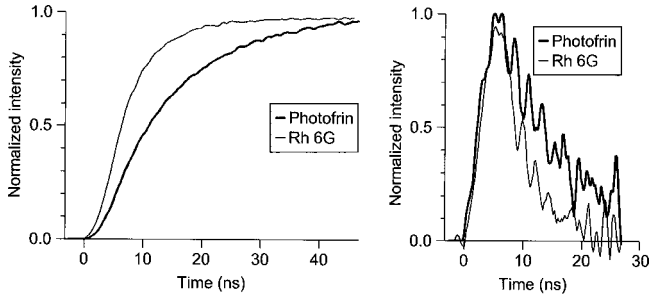

FIG. 2. Curves illustrating the time resolution of the system. The integrated signal from Photofrin and rhodamine 6 G as a function of the gate width (left panel), and the corresponding differentiated and normalized curves (right panel).

III. RESULTS

In the sensitivity studies using the fluorescence intensity standard as a sample, we obtained fluorescence peak intensities of about 50 000 counts per laser pulse using gain setting 2 of the intensified CCD camera. Gain setting 2 means that 11.3 counts are recorded by the CCD per photoelectron generated in the photocathode of the intensifier. This gain was chosen for both excitation wavelengths to record a signal slightly below the level for detector saturation. The signal-to-noise (S/N) ratio in the peak was about 100 for 337 nm excitation and 90 for 405 nm excitation. The measurements of the skin using gain setting 6 (115 counts per photoelectron) resulted in corresponding S/N ratios of 24 and 29. The noise in a typical background recording for a single readout at gain 6 was typically 150 counts, yielding a dynamic range of the system of approximately 500 for single-pulse measurements.

Curves illustrating the time-resolution of the system are shown in the left part of Fig. 2. The upper curve for Rh6G, having a short lifetime, was obtained by measuring the fluorescence intensity as a function of gate width of the detector. The fluorescence intensity recorded from the Photofrin sample exhibiting a long fluorescence lifetime, increases much slower than the curve obtained from Rh6G. This can also be seen in the differentiated curves (both normalized to unity for clarity) presented in the right-hand part of Fig. 2. The rise time of both curves, illustrating the system response, is about 4 ns, where the effects of trigger jitter are also included.

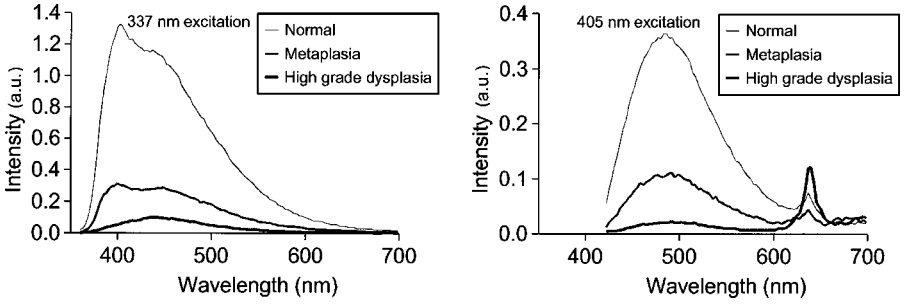

FIG. 3. Time-integrated fluorescence spectra from measurements of normal tissue, metaplasia, and high grade dysplasia in the colon following excitation at 337 nm (left panel) and 405 nm (right panel). The patient investigated in the panel to the right had received ALA at a dose of 5 mg/kg body weight.

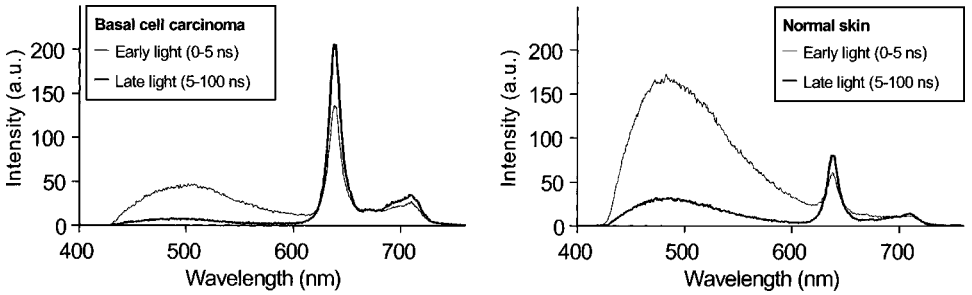

FIG. 4. Time-resolved fluorescence spectra recorded in a basal cell carcinoma (left panel) and the adjacent normal skin (right panel) following 4 h topical application of ALA.

A. Clinical evaluation

The functionality of the system in clinical work has been evaluated in investigations of lesions *in vivo* in three different clinical specialties. The first investigation was performed to assess the potential of laser-induced fluorescence spectroscopy to distinguish between hyperplastic and adenomatous polyps in the colon.[41] Time-integrated fluorescence spectra excited at 337 nm from three locations in the colon of one patient are shown to the left in Fig. 3. The curve with the highest intensity is recorded from the normal colonic mucosa, while the second most intense curve is measured from a metaplastic polyp and the third curve originates from an adenomatous polyp with high-grade dysplasia. The reduction in the intensity of blue fluorescence in abnormal tissue is a common feature, very valuable for diagnostics. Similar time-integrated spectra excited at 405 nm from another patient, who had received a low dose of 5 mg per kilogram body weight ALA per oz prior to the examination, are shown to the right-hand side in Fig. 3. The protoporphyrin IX (PpIX) signal at about 635 nm becomes more prominent in the malignant tissue, which again also has a reduced blue fluorescence.

In the second study, fluorescence spectroscopy was used for characterizing cardiovascular lesions. Spectra excited at 337 nm recorded from a patient undergoing coronary bypass surgery were recorded. The spectra showed a sharp dip at about 415 nm due to blood reabsorption. It has previously been shown that atherosclerotic plaque differs spectroscopically substantially from normal vessel wall (see, e.g., Ref. 26).

Time-resolved spectra recorded from a basal cell carcinoma in the skin next to the eye, as well as from the normal surrounding skin, in a woman with Caucasian skin type are shown in Fig. 4. ALA was administered topically in a cream for a period of 4 h before the examination. This application resulted in a haem-cycle production of PpIX. The 100-nm-long gate with fast switch on and off times (see Fig. 2, right panel) was first placed early to only include the first 5 ns of the fluorescence decay. Then the gate was moved forward so that the leading edge of the gate replaced the earlier position of the trailing edge. Thus late fluorescence, starting 5 ns after the fluorescence onset, was collected. The PpIX molecules exhibit a long fluorescence lifetime, much longer than the one for the tissue autofluorescence, and is thus better pronounced in the spectra with the late gate. The autofluorescence in the region between 450 and 600 nm, having a short lifetime, is accordingly reduced in the late gate.

Figure 5 shows some sample spectra from diffusely scattered white light, recorded with the system. The distance between the source and the detection fibers was 1 mm (center to center). The curves have been normalized to the signal recorded from a 99% reflectance standard (Oriel Instruments, SRS-99-010). Measurements on locations with high blood perfusion, such as the lip and the fingertip, show a clear imprint of the absorption spectrum of oxy-hemoglobin. This can be seen as the two dips in the wavelength range between 500 and 600 nm. On the lower arm, however, this spectral signature was not obvious.

IV. DISCUSSION

In the design of the system presented, the main goal was to develop a very compact fluorosensor for clinical use that should be fully computer controlled to enable rapid recordings and should have a user interface allowing the use by nonspecialists. Compact parts, several partly custom redesigned, were chosen. Despite the requirements of a small system with a simple user interface, the fluorosensor has become flexible with a sophisticated spectroscopic potential. It provides time-gated emission spectra at two excitation wavelengths in a rapid sequence of measurements, all fully computer controlled. Another benefit of the compact design is the short light paths inside the system, resulting in minimal light losses.

The use of two excitation wavelengths can be favorable to optimize the potential for tissue characterization utilizing

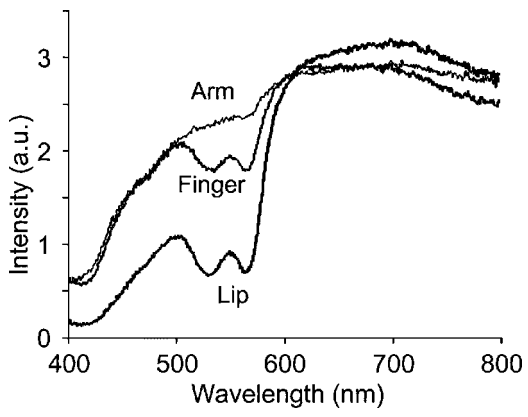

FIG. 5. Reflectance spectra of three types of human skin.

both the tissue autofluorescence and the fluorescence from an externally administrated marker. Another potential use of two excitation wavelengths is to more accurately determine the concentration of a fluorophore inside the tissue, by minimizing the influences of the absorption and scattering properties of the tissue through appropriate data processing.[42,43] Further information on the tissue optical properties that can be used for more accurate concentration measurements can be assessed from recordings of diffusely scattered white light.

ACKNOWLEDGMENTS

The assistance from Åke Bergquist and Göran Werner in the design and implementation of the system is gratefully acknowledged, as is the collaboration with the Endoscopy section at the Department of Internal Medicine at the Karolinska Hospital, the Department of Vascular Surgery at the London Royal Hospital, and the Department of Oncology at the Lund University Hospital, as well as with Charlotta Eker and Sara Pålsson in collecting the clinical data presented as illustrations of the system performance. The work was supported by the Swedish National Board for Industrial and Technical Development, the Knut and Alice Wallenberg Foundation, the Swedish Foundation for Strategic Research, and the European Commission (Grant No. BMH4-96-0320).

[1] R. L. Lipson, E. J. Baldes, and A. M. Olsen, J. Thorac. Cardiovasc. Surg. **42**, 623 (1961).
[2] A. E. Profio and D. R. Doiron, Phys. Med. Biol. **22**, 949 (1977).
[3] Y. Yang, Y. Ye, F. Li, Y. Li, and P. Ma, Lasers Surg. Med. **7**, 528 (1987).
[4] C. R. Kapadia, F. W. Cutruzzola, K. M. O'Brien, M. L. Stetz, R. Enriquez, and L. I. Deckelbaum, Gastroenterology **99**, 150 (1990).
[5] S. Andersson-Engels, Å. Elner, J. Johansson, S.-E. Karlsson, L. G. Salford, L.-G. Strömblad, K. Svanberg, and S. Svanberg, Lasers Med. Sci. **6**, 415 (1991).
[6] R. Richards-Kortum, R. P. Rava, R. E. Petras, M. Fitzmaurice, M. Sivak, and M. S. Feld, Photochem. Photobiol. **53**, 777 (1991).
[7] K. T. Schomacker, J. K. Frisoli, C. C. Compton, T. J. Flotte, J. M. Richter, N. S. Nishioka, and T. F. Deutsch, Lasers Surg. Med. **12**, 63 (1992).
[8] T. Vo-Dinh, M. Panjehpour, B. Overholt, C. Farris, P. Buckley III, and R. Sneed, Lasers Surg. Med. **16**, 41 (1995).
[9] N. Ramanujam, M. F. Mitchell, A. Mahadevan, S. Thomsen, A. Malpica, T. Wright, N. Atkinson, and R. Richards-Kortum, Lasers Surg. Med. **19**, 63 (1996).
[10] G. Zonios, R. Cothren, J. M. Crawford, M. Fitzmaurice, R. Manoharan, J. van Dam, and M. S. Feld, Ann. N.Y. Acad. Sci. **838**, 108 (1998).
[11] U. Gustafsson, S. Pålsson, and S. Svanberg, Rev. Sci. Instrum. **71**, 3004 (2000).
[12] S. Montán, K. Svanberg, and S. Svanberg, Opt. Lett. **10**, 56 (1985).
[13] T. Hirano, M. Ishizuka, K. Suzuki, K. Ishida, S. Suzuki, S. Miyaki, A. Honma, M. Suzuki, K. Aizawa, H. Kato, and Y. Hayata, Lasers Life Sci. **3**, 99 (1989).
[14] B. Palcic, S. Lam, J. Hung, and C. MacAulay, Chest **99**, 742 (1991).
[15] M. Kriegmair, R. Baumgartner, R. Knuechel, P. Steinbach, A. Ehsan, W. Lumper, F. Hofstädter, and A. Hofstetter, Urology **44**, 836 (1994).
[16] D. Frimberger, D. Zaak, H. Stepp, R. Knuchel, R. Baumgartner, P. Schneede, N. Schmeller, and A. Hofstetter, Urology **58**, 372 (2001).
[17] D. Zaak, M. Kriegmair, H. Stepp, R. Baumgartner, R. Oberneder, P. Schneede, S. Corvin, D. Frimberger, R. Knuchel, and A. Hofstetter, Urology **57**, 690 (2001).
[18] A. Ehsan, F. Sommer, G. Haupt, and U. Engelmann, Urol. Int. **67**, 298 (2001).
[19] Z. Malik, M. Dishi, and Y. Garini, Photochem. Photobiol. **63**, 608 (1996).
[20] D. P. Ladner, R. A. Steiner, J. Allemann, U. Haller, and H. Walt, Br. J. Cancer **84**, 33 (2001).
[21] G. A. DuVall, R. Saidi, J. Kost, D. Scheider, L. Lilge, M. Cirocco, S. Hassaram, G. Kandel, P. Kortan, G. Haber, T. Mang, R. DaCosta, B. C. Wilson, and N. Marcon, Gastrointest. Endosc. **45**, 14 (1997).
[22] K. Svanberg, I. Wang, S. Colleen, I. Idvall, C. Ingvar, R. Rydell, D. Jocham, H. Diddens, S. Bown, G. Gregory, S. Montán, S. Andersson-Engels, and S. Svanberg, Acta Radiol. **39**, 2 (1998).
[23] Y. Kusunoki, F. Imamura, H. Uda, M. Mano, and T. Horai, Chest **118**, 1776 (2000).
[24] M. Kobayashi, H. Tajiri, E. Seike, M. Shitaya, S. Tounou, M. Mine, and K. Oba, Cancer Lett. **165**, 155 (2001).
[25] R. Cubeddu, F. Docchio, W. Q. Liu, R. Ramponi, and P. Taroni, Rev. Sci. Instrum. **59**, 2254 (1988).
[26] S. Andersson-Engels, J. Johansson, U. Stenram, K. Svanberg, and S. Svanberg, IEEE J. Quantum Electron. **26**, 2207 (1990).
[27] R. Cubeddu, G. Canti, P. Taroni, and G. Valentini, Lasers Med. Sci. **12**, 200 (1997).
[28] R. Jones, K. Dowling, M. J. Cole, D. Parsons-Karavassilis, M. J. Lever, P. M. W. French, J. D. Hares, and A. K. L. Dymoke-Bradshaw, Electron. Lett. **35**, 256 (1999).
[29] A. E. Profio, Proc. SPIE **1426**, 44 (1991).
[30] S. Andersson-Engels and B. C. Wilson, J. Cell Pharmacol. **3**, 48 (1992).
[31] T. G. Papazoglou, J. Photochem. Photobiol., B **28**, 3 (1995).
[32] I. J. Bigio and J. R. Mourant, Phys. Med. Biol. **42**, 803 (1997).
[33] S. Andersson-Engels, C. af Klinteberg, K. Svanberg, and S. Svanberg, Phys. Med. Biol. **42**, 815 (1997).
[34] G. A. Wagnières, W. M. Star, and B. C. Wilson, Photochem. Photobiol. **68**, 603 (1998).
[35] M. A. Scott, C. Hopper, A. Sahota, R. Springett, B. W. Mcllroy, S. G. Bown, and A. J. MacRobert, Lasers Med. Sci. **15**, 63 (2000).
[36] R. A. Drezek, R. Richards-Kortum, M. A. Brewer, M. S. Feld, C. Pitris, A. Ferenczy, M. L. Faupel, and M. Follen, Br. J. Cancer Suppl. **98**, 2015 (2003).
[37] S. Andersson-Engels, K. Svanberg, and S. Svanberg, in *Biomedical Optics*, edited by J. Fujmoto (Plenum, New York, to be published).
[38] J. Ankerst, S. Montán, K. Svanberg, and S. Svanberg, Appl. Spectrosc. **38**, 890 (1984).
[39] W. Alian, S. Andersson-Engels, K. Svanberg, and S. Svanberg, Br. J. Cancer **70**, 880 (1994).
[40] R. Cubeddu, R. Ramponi, and G. Bottiroli, Chem. Phys. Lett. **128**, 439 (1986).
[41] C. Eker, S. Montán, E. Jamarillo, K. Koizumi, S. Andersson-Engels, K. Svanberg, S. Svanberg, and P. Slezak, Gut **44**, 511 (1999).
[42] M. Sinaasappel and H. J. C. M. Sterenborg, Appl. Opt. **32**, 541 (1993).
[43] A. Bogaards, M. C. G. Aalders, A. J. L. Jongen, E. Dekker, and H. J. C. M. Sterenborg, Rev. Sci. Instrum. **72**, 3956 (2001).